Undrained monotonic and cyclic torsional simple shear behavior of the Aso pumiceous soil deposits

G. Chiaro
Department of Civil and Natural Resources Engineering, University of Canterbury, Christchurch, New Zealand

T. Kiyota & M. Umar
Institute of Industrial Science, University of Tokyo, Tokyo, Japan

ABSTRACT: The Takanodai landslide was a mobile earth slide caused by the 2016 Kumamoto earthquakes. Field observations suggested that the soil to cause the slope failure could be a thin layer of Aso pumice soil sandwiched between two layers of clay volcanic ashes. However, there exist debates among researchers about the actual failure mechanisms. In an attempt to provide new insights into this problem, this paper reports on preliminary results of monotonic and cyclic undrained torsional simple shear tests carried out on reconstituted specimens of Aso pumice. The test results confirmed that Aso pumice has the tendency to suddenly lose its shear strength and develop flow-type large shear strain exceeding 50% when subjected to both monotonic and cyclic torsional simple shear loading conditions. Moreover, in addition to high inertial stresses, it is the presence of an initial driving shear stress that significantly contributes to the flow-type failure and associated large deformation.

1 INTRODUCTION

Between April 14th and 16th, 2016, a series of powerful earthquakes including a major event of moment magnitude (M_w) 7.0 and two major foreshocks (M_w 6.2 and M_w 6.0) hit the Island of Kyushu, Japan. The earthquakes known as the 2016 Kumamoto Earthquakes, contributed to major devastation in Kumamoto City, Mashiki Town and in the mountainous areas of the Mount Aso Volcanic Caldera (Dang et al., 2016; Mukunoki et al., 2016; Kiyota et al., 2017; Chiaro et al., 2017a). In the Mount Aso Volcanic Caldera, medium to large scale landslides and rock falls were frequently observed. Among many landslides, the earthquakes caused the failure of a gentle slope near the Aso Volcanological Laboratory of Kyoto University. This large-scale runout slope failure, known as the Takanodai landslide (Dang et al., 2016; Mukunoki et al., 2016), destroyed at least 7 houses and killed 5 people, threatened many other houses and blocked several roads (Figure 1a).

Field observations indicated that the Takanodai landslide was a mobile earth slide that developed into a flow-type slide on a low angle slope (around 10-15^o), with a travel angle from landslide crown to debris toe of approximately 6^o (Figure 1b). As shown in Figure 1a, the landslide travelled in three different directions from a common source. The landslide was about 100 m in width, 300-600 m in length and 5-10 m in depth. Relatively large intact blocks of soil, grass and trees (Photo 1) travelled towards the toe of the slope suggesting a translational movement of the soil. Tension cracks and scarps above the head scarp adjacent to the Aso Volcanological Laboratory were widely observed, indicating the potential for head scarp retrogression and/or new incipient landslides to occur. As shown in Photo 2, the slip surface was identified and traces of orange-colored pumice soil were clearly noted on it.

Field surveys also suggested that the key soil to cause the slope failure could be the orange-colored pumice soil deposit (Mukunoki et al., 2016; Chiaro et al., 2017a). Moreover, the sensitivity ratio of shear strength of this volcanic soil before and after the earthquakes as well as the water

pressure buildup could be the cause for the flow type slope failure. Nevertheless, there is much discussion among researchers about the actual failure mechanisms. Therefore, further site investigations, including detailed laboratory studies and numerical investigations are required to clarify the mechanisms for such a flow-type failure of a gentle slope (Chiaro et al., 2018). In this paper, in an attempt to provide new insights into this problem, preliminary results of monotonic and cyclic undrained torsional simple shear tests carried out on reconstituted specimens of Aso pumice are presented and discussed.

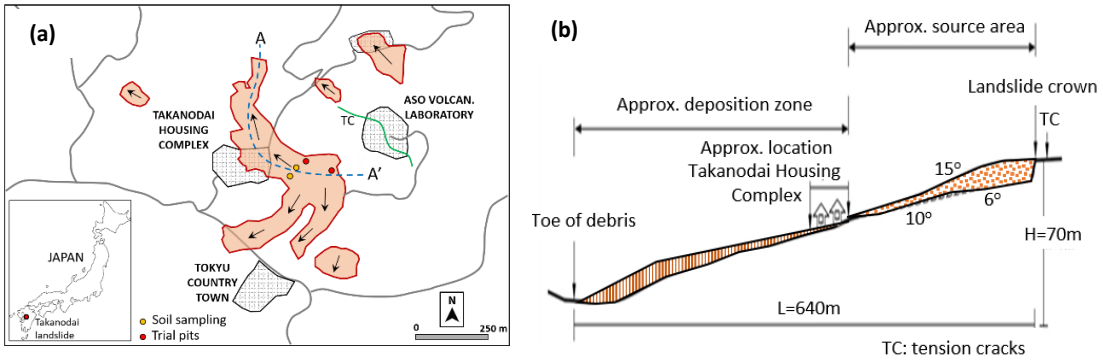

Figure 1. The Takanodai landslide: (a) plan view; and (b) cross-section A-A'.

Photos: (1) The Takanodai landslide – looking uphill; and (2) Slip surface with traces of Aso pumice soil.

2 TEST APPARATUS, MATERIAL AND PROCEDURE

2.1 Test apparatus

Laboratory testing was carried out using the fully automated torsional apparatus shown in Figure 2, which has been developed in the Institute of Industrial Science, University of Tokyo (Kiyota et al., 2008). Such a device is capable of achieving double amplitude shear strain levels exceeding 50% by using a belt-driven torsional loading system that is connected to an AC servo motor through electro-magnetic clutches and a series of reduction gears. Torque moment and axial load are measured by a two-component load cell, which is installed inside the pressure cell. Difference in pressure levels between the cell pressure and the pore water pressure are measured by a high-capacity differential pressure transducer (HCDPT). On the other hand, volume change during the consolidation process is measured by a low-capacity differential pressure transducer (LCDPT). A potentiometer with a wire and a pulley is employed to measure the rotation angle of the top cap and, thus, the large torsional deformation. Shear stress amplitude is controlled by a computer, which monitors the outputs from the load cell, computes the corresponding stress value and controls the device accordingly. It should be note that the measured shear stress is corrected for the effects of the membrane force by using the hyperbolic equation proposed by Chiaro et al. (2017c).

In using a hollow cylinder torsional shear apparatus, four independently loading components, namely vertical axial load (F_z), torque load (T), inner cell pressure (p_i) and outer cell pressure (p_o) can be applied. The correspondent stress components i.e. axial stress (σ_z), radial stress (σ_r), circumferential stress (σ_θ) and torsional shear stress ($\tau_{z\theta}$) can be defined as follows (Hight et al., (1983):

$$\sigma_z = \frac{F_z}{\pi(r_o^2 - r_i^2)} + \frac{(p_o r_o^2 - p_i r_i^2)}{(r_o^2 - r_i^2)}, \quad \sigma_r = \frac{(p_o r_o + p_i r_i)}{(r_o + r_i)}, \quad \sigma_\theta = \frac{(p_o r_o - p_i r_i)}{(r_o - r_i)}, \quad \tau = \tau_{z\theta} = \frac{3T}{2\pi(r_o^3 - r_i^3)} \tag{1}$$

where r_o and r_i are the outer and inner radius of the specimen, respectively.

On the other hand, the average torsional shear strain is defined as:

$$\gamma = \gamma_{z\theta} = \frac{2\theta}{3H} \frac{(r_o^3 - r_i^3)}{(r_o^2 - r_i^2)} \tag{2}$$

where θ is the circumferential angular displacement and H is the specimen height.

The average principal stresses σ_1 (major), σ_2 (intermediate), σ_3 (minor) as well as the mean principal stress p are given by:

$$\begin{Bmatrix} \sigma_1 \\ \sigma_3 \end{Bmatrix} = \frac{\sigma_z + \sigma_\theta}{2} \pm \sqrt{\left(\frac{\sigma_z - \sigma_\theta}{2}\right)^2 + \tau_{z\theta}^2}, \quad \sigma_2 = \sigma_r, \quad p = \frac{\sigma_1 + \sigma_2 + \sigma_3}{3} \tag{3}$$

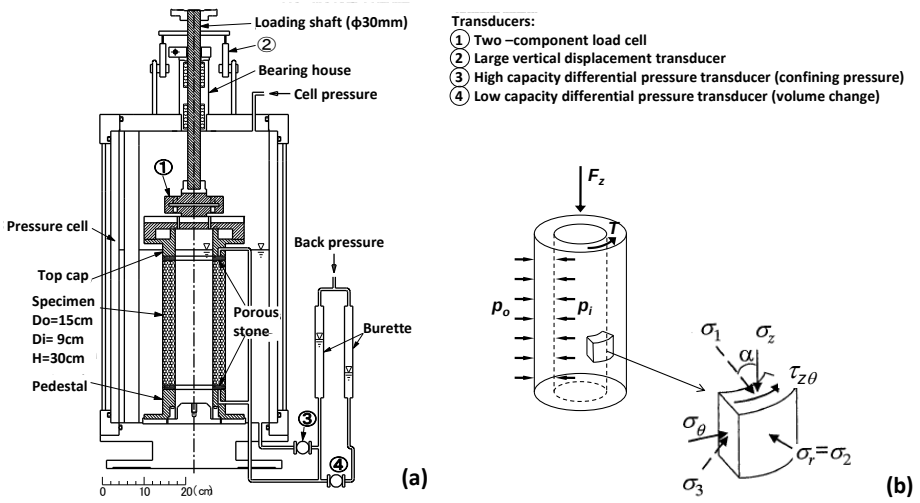

Figure 2. (a) Torsional shear apparatus used in this study (adopted from Kiyota et al., 2008); and (b) External forces and stress components acting on a hollow cylindrical specimen (Chiaro et al., 2017b).

2.2 Test material

All the tests were performed on Aso pumice soil samples collected from the Takanodai landslide investigation site (see sampling location in Figure 1a). Aso pumice had an in-situ dry density of 0.6 g/cm^3, a natural water content of 117% and a specific gravity of 2.3 (average value). Particle size distribution (PSD) curve and Scanning Electron Microscope (SEM) photos are shown in Figure 3. It is a sensitive weathered pyroclastic soil that contain silt and sand grains in a semi-continuous anisotropic matrix. There is some halloysite present as matrix material in this soil sample; overall, the structure of this soil is much more dependent on contacts between matrix material rather than silt and sand.

2.3 Specimens preparation method and testing procedure

Similar to other volcanic soils, Aso pumice soil has a highly varying specific gravity of individual grains caused by occluded air pockets. Accordingly, conventional specimen preparation methods are not suitable (Hyodo et al., 1998). For instance, in the case of water pluviation volcanic soils tend to segregate, with some grains floating on the water surface. Using the wet tamping method, crushing of particles may become very significant. Air pluviation also has been found to be problematic. By trial and error, in this study, the following procedure was found most appropriate to build hollow cylindrical specimens with uniform density. To minimize particle crushing during specimen preparation, each specimen was prepared in 15 layers of equal height by spooning the soil (prepared at its natural water content) into the mold and subsequently applying very gentle tamping until a target density was achieved.

Due to high internal void ratio, saturation of volcanic soil requires a rigorous de-airing process (Hyodo et al., 1998; Pender et al., 2006). In this study, therefore, the double vacuum method (Ampadu, 1991) was employed before and during percolation of water into the specimen. By doing so, and applying a back pressure of 200 kPa, a high degree of saturation was ensured i.e. Skempton's 'B' values were greater than 0.95. After completing the saturation process, the specimens were isotropically consolidated by increasing the effective mean stress state (p_0') up to 100 kPa, which is representative of the in-situ stress conditions (Chiaro et al., 2018b).

Because of the small amount of soil available, only four hollow cylindrical specimens with dimension of 150 mm outer diameter, 90 mm inner diameter and 300 mm height were tested. As summarized in Table 1, strain-controlled (shear strain rate of 0.5 %/min) cyclic and monotonic undrained torsional simple shear tests were performed. In the case of cyclic tests, the loading direction was reversed when the amplitude of shear stress reached the target value. Whereas, in the monotonic test Aso #2, the static shear corresponding to the in-situ sloping stress condition (i.e. shear stress component induced by slope inclination) was applied by means of drained monotonic torsional shear loading before undrained monotonic shearing (Chiaro et al., 2012). In all the tests, during the undrained shearing phase, the vertical displacement of the top cap was mechanically prevented with the aim to simulate as much as possible the simple shear condition that ground undergoes during horizontal seismic excitations.

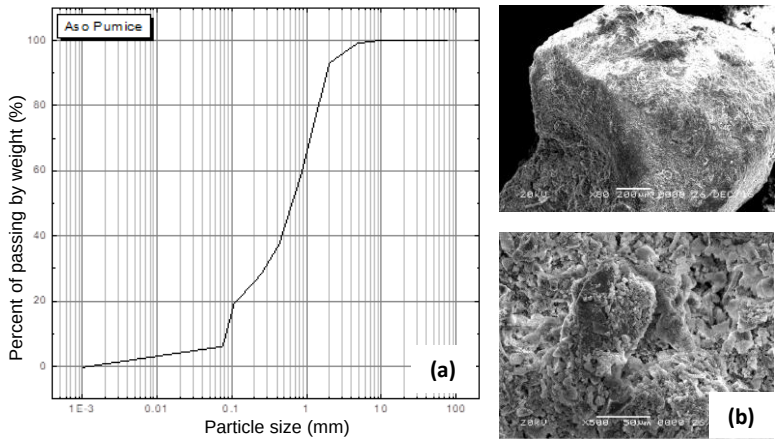

Figure 3. Aso pumice: (a) particle size distribution curve; and (b) SEM photos.

Table 1. List of undrained cyclic torsional simple shear tests performed in this study.

Test	Type	Dry density (g/cm^3)	Shear stresses (kPa)		Effective mean stress (kPa)
			Cyclic shear	Static shear	
Aso #1	Monotonic	0.56	--	0	100
Aso #2	Monotonic	0.60	--	25	97
Aso #3	Cyclic	0.63	20	0	100
Aso #4	Cyclic	0.58	25	0	98

3 TEST RESULTS AND DISCUSSIONS

3.1 Undrained monotonic torsional simple shear test

Figure 4 shows the results of the monotonic test Aso #1, in terms of effective stress path and stress-strain relationship. For the sake of comparison, typical monotonic torsional shear behavior of a very loose Toyoura sand specimen is also illustrated in the same figure. As shown by Figure 4a, under the stress conditions used in this study, Aso pumice soil exhibited a purely contractive behavior, during which the mean effective stress (p') decreases while shear stress (τ) progressively increases up to a transient peak stress (in correspondence of the instability line or IL line;

Lade, 1993). The peak stress state is accompanied by unstable behavior with a sudden loss of strength and large development of pore water pressure and shear strain. In addition, by looking at the stress-strain responses (Figure 5b), strain-softening behavior (i.e. decrease in shear strength owing to shear strain increase) can be observed after the transient peak stress. Moreover, Aso pumice soil showed a tendency to deform under a nearly constant stress (residual shear strength).

Although Aso pumice has the tendency to experience flow-type failure, when compared with the response of loose Toyoura sand (D_r = 25%) that also experienced flow-type failure liquefaction, some key differences can be found. For instance, typically flow failure in loose sands is associated with the development of full liquefaction (zero-*p*' stress state), at which state soil completely lose its shear strength and stiffness. However, in the case of Aso pumice, flow failure occurs under a nearly constant residual shear strength; this behavior is often observed in sensitive clay-like soil rather than sands. However, as mentioned earlier, there is some halloysite present as matrix material in this soil sample and the structure of this soil is much more dependent on contacts between matrix material rather than silt and sand. Moreover, the high crushability of Aso pumice grains (crushable volcanic soil) compared to that of sand particles (hard grained material) may play an important role on the observed mechanical response.

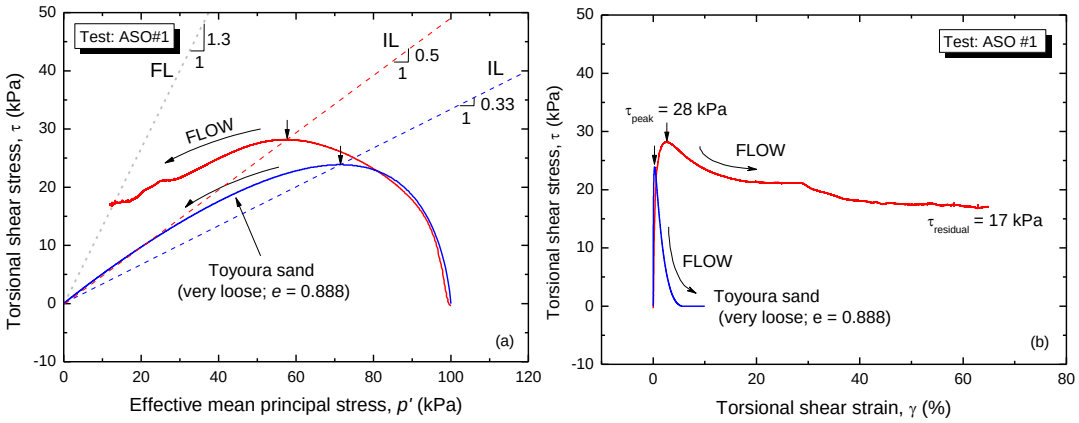

Figure 4. Comparison between the undrained monotonic behavior of Aso pumice (Test Aso #1) and that of very loose Toyoura sand (Chiaro et al., 2013b).

3.2 Undrained monotonic torsional simple shear test with initial static shear

In order to investigate the effects of slope inclination on the undrained response of Aso pumice soil, a specimen was pre-sheared by applying 25 kPa of initial static shear (Figure 5). The overall, behavior of Aso pumice soil subjected to monotonic shearing loading did not change significantly, in the sense that it remained purely contractive and strain-softening followed by large strain development was observed after the peak stress state. However, an increase in both the peak shear strength and the residual strength was noticed.

It is important to mention that, this test (ASO #2) indicated that the residual shear strength of Aso pumice under sloping conditions was 27 kPa; that is not much greater that the driving shear stress (25 kPa) induced by the slope inclination. This may imply that the presence of a driving shear stress in conjunction with high and repeated inertial stresses may have been the key triggering conditions for the flow-type failure and large deformation of Aso pumice observed at the Takanodai landslide site.

3.3 Undrained monotonic torsional simple shear test with initial static shear

Undrained shear tests were performed using two levels of cyclic stress ratio (CSR = τ_{cyclic}/p_0') of 0.20 and 0.25. Figures 6 and 7 show the effective stress paths with their associate stress-strain plots. In both tests, Aso pumice soil exhibited a cyclic mobility failure type where the effective stress path progressively moves toward the zero-*p*' conditions but the cyclic shear strain increases up to large values. In particular, initially the shear strain were very small and then suddenly exceed values of double amplitude shear strain (γ_{DA}) of 50% or more during the last few cycles of loading

as *p*' approached zero. Hyodo et al. (1998) presented similar behavior for the crushable Shirasu soil (a volcanic soil from southern Kyushu) subjected to cyclic triaxial shearing.

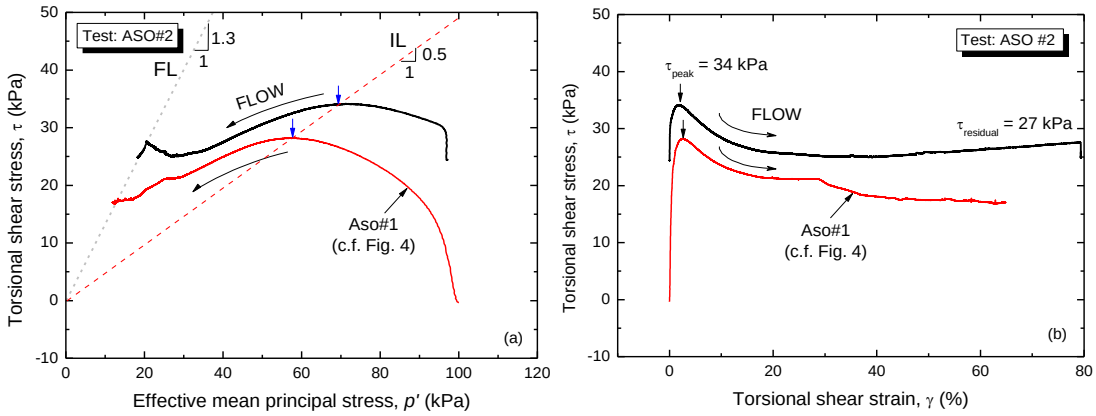

Figure 5. Results of monotonic undrained torsional simple shear test with initial static shear (ASO#2).

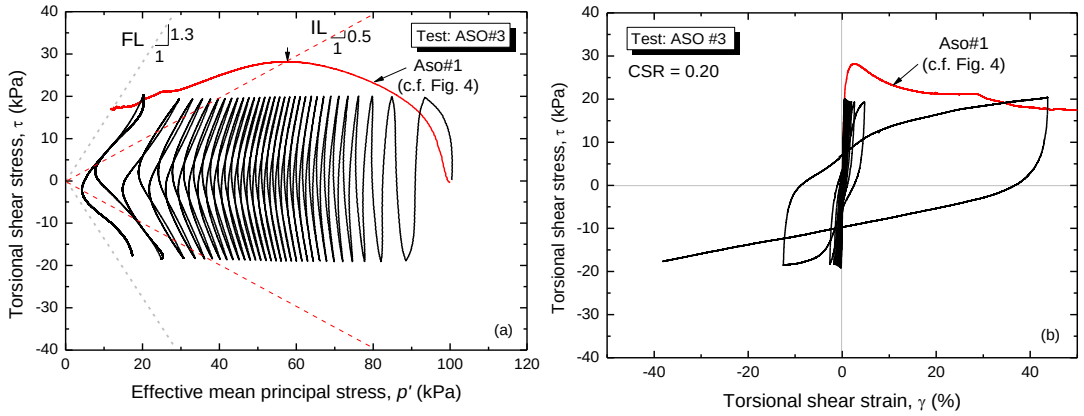

Figure 6. Cyclic undrained torsional shear behavior of Aso Pumice subjected to a CSR = 0.20.

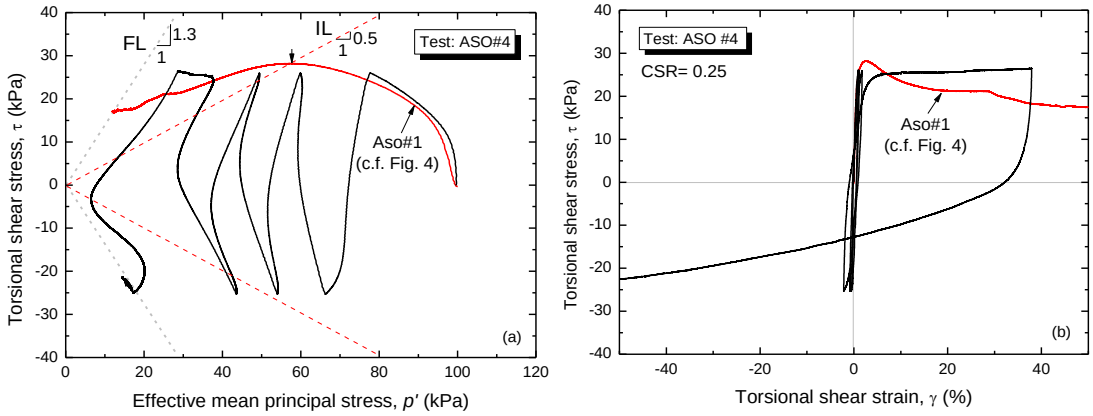

Figure 7. Cyclic undrained torsional shear behavior of Aso Pumice subjected to a CSR = 0.25.

3.4 Specimen deformation

For completeness, the deformation characteristics of Aso pumice specimen at various states of shearing during Test ASO #3 are shown in Photo 3. At stage 2, corresponding to a single amplitude shear strain (γ_{SA}) of about 7.5%, the deformation was uniform throughout the specimen

height. At stage 3 (γ_{SA} = 15%), the deformation was still rather uniform. However, at stage 4 (γ_{SA} = 30%), it appears that strain localization started to develop in the upper part of the specimen.

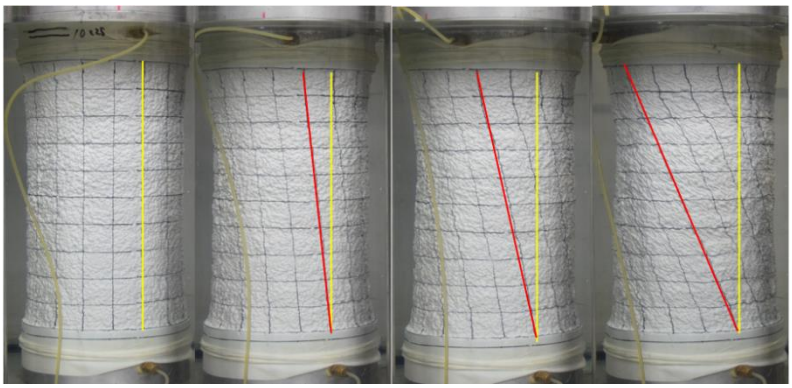

Stage 1 (γ_{SA} = 0%) | Stage 2 (γ_{SA} = 7.5%) | Stage 3 (γ_{SA} = 15%) | Stage 4 (γ_{SA} = 30%)

Photo 3. Typical deformation of Aso pumice specimens in cyclic undrained torsional shear tests.

3.5 Resistance against cyclic strain accumulation

Conventionally, the resistance to liquefaction or to cyclic strain accumulation of soils is evaluated as the number of cycles to develop a specific amount of double amplitude shear strain (γ_{DA}) during cyclic loading. Accordingly, Figure 8 reports the liquefaction resistance of Aso pumice soil corresponding to a double amplitude shear strain (γ_{DA}) of 7.5%, which is equivalent to a double amplitude shear strain of 5% in triaxial tests. In the same figure, liquefaction resistances of Toyoura sand and Christchurch sand (both hard grained soils) are reported for comparison.

Despite the differences in cyclic behavior previously described, it appears that the liquefaction resistance of crushable Aso Pumice soil can be closely related to that of less-crushable medium-dense sandy soils.

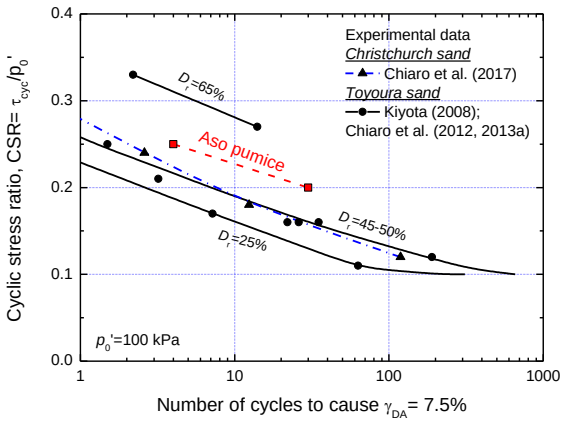

Figure 8. Cyclic strength curve of Aso pumice (for 7.5% double amplitude shear strain) and its comparison with those of Toyoura sand and Christchurch sand.

4 CONCLUSIONS

Following reconnaissance damage surveys, a thin deposit of crushable pumice soil was understood to be responsible for the Takanodai landslide occurred during the 2016 Kumamoto earthquakes, Japan. However, there were discussions in regards to the potential failure mechanisms.

Therefore, in an attempt to provide insights into the failure mechanisms of the Takanodai landslide, several monotonic and cyclic undrained torsional simple shear tests were carried out in this study on reconstituted specimens of Aso pumice soil.

The test results revealed that Aso pumice soil has the tendency to show a post-peak flow-type failure behavior characterized by an abrupt develop of large shear strains exceeding 50% or more when subjected to monotonic torsional shear loadings. On the contrary, under cyclic shear stress condition, a progressive build-up of excess pore water pressure was observed until the stress state reached the failure envelop. It was followed by a flow-type failure with a rapid development of large shear strains. More importantly, in addition to high inertial stresses, it is the presence of an initial driving shear stress that significantly contributed to the observed flow-type failure and associated large deformation.

5 REFERENCES

Ampadu, S.I.K. 1991. Undrained behavior of kaolin in torsional simple shear, *Ph.D. Thesis*, Dept. of Civil Engineering, University of Tokyo, Japan.

Chiaro, G., Alexander, G., Brabhaharan, P., Massey C., Koseki J., Yamada, S. & Aoyagi, Y. 2017. Reconnaissance report on geotechnical and geological aspects of the 2016 Kumamoto Earthquake, Japan, *Bulletin of the New Zealand Society for Earthquake Engineering* 50(3): 365-393.

Chiaro G., De Silva L.I.N. & Koseki J. 2017. Modeling the effects of static shear on the undrained cyclic torsional simple shear behavior of liquefiable sand. *Geotechnical Engineering Journal* 48(4): 1-9.

Chiaro, G., Kiyota, T. & Koseki, J. 2013a. Strain localization characteristics of loose saturated Toyoura sand in undrained cyclic torsional shear tests with initial static shear. *Soils and Foundations* 53: 23-34.

Chiaro, G., Kiyota, T. & Miyamoto, H. 2017. Liquefaction potential and large deformation properties of Christchurch liquefied sand subjected to undrained cyclic torsional simple shear loading. *Proc. 19th Int. Conf. Soil Mechanics and Geotechnical Engineering*, Seoul, South Korea, 1497-1500.

Chiaro, G., Koseki, J. & De Silva, L.I.N. 2013b. A density- and stress-dependent elasto-plastic model for sands subjected to monotonic torsional shear loading. *Geotechnical Engineering Journal* 44(2): 18-26.

Chiaro, G., Koseki, J. & Sato, T. 2012. Effects of initial static shear on liquefaction and large deformation properties of loose saturated Toyoura sand in undrained cyclic torsional shear. *Soils and Foundations* 52(3): 498-510.

Chiaro, G., Umar, M., Kiyota, T. & Massey, C. 2018b. The Takanodai landslide, Kumamoto, Japan: insights from post-earthquake field observations, laboratory tests and numerical analyses. *ASCE Geotechnical Special Publication* 293: 98-111.

Dang, K., Sassa, K., Fukuoka, H., Sakai, N., Sato, Y., Takara, K., Quang, L.H., Loi, D.H., Tien, P.V. & Ha, N.D. 2016. Mechanism of two rapid and long runout landslides in the 16 April 2016 Kumamoto earthquake using a ring-shear apparatus and computer simulation. *Landslides* 13(6): 1525–1534.

Hight, D.W., Gens, A. & Symes, M.J. 1983. The development of a new hollow cylinder apparatus for investigating the effects of principal stress rotation in soils. *Geotechnique* 33: 355-383.

Hyodo, M., Hyde, A.F.L. & Aramaki, N. 1998. Liquefaction of crushable soils. *Geotechnique* 48: 527-543.

Kiyota, T., Sato, T., Koseki, J. & Mohammad, A. 2008. Behavior of liquefied sands under extremely large strain levels in cyclic torsional shear tests. *Soils and Foundations* 48(5), 727-739.

Kiyota, T., Ikeda, T., Konagai, K. & Shiga, M. 2017. Geotechnical damage caused by the 2016 Kumamoto Earthquake, Japan. *International Journal of Geoengineering Case Histories* 4(2): 78-95.

Lade, P.V. 1993. Initiation of static instability in the submarine Nerlerk berm, *Canadian Geotechnical Journal*, 30(6): 895-904.

Mukunoki, T., Kasama, T., Murakami, S., Ikemi, H., Ishikura, R., Fujikawa, T., Yasufuka, N. & Kitazono, Y. 2016. Reconnaissance report on geotechnical damage caused by an earthquake with JMA seismic intensity 7 twice in 28h, Kumamoto, Japan. *Soils and Foundation* 56(6): 947-964.

Pender, M.J., Wesley, L.D., Larkin, T. J. & Pranjoto, S. 2006. Geotechnical properties of a pumice sand. *Soil and Foundations* 46(1), 69-81.